

DESIGN, ACOUSTIC PERFORMANCE AND ADDITIVE MANUFACTURING OF HELICOPTER ROTOR BLADES WITH UNCONVENTIONAL SHAPES

Gabriela-Alexandra Badicu¹, Sebastian-Marian Zaharia², Mihai Alin Pop³

¹ Transilvania University of Brasov, gabriela.badicu@student.unitbv.ro

² Transilvania University of Brasov, zaharia_sebastian@unitbv.ro

³ Transilvania University of Brasov, mihai.pop@unitbv.ro

ABSTRACT: In this paper, a blade with unconventional structure, corrugations and BERP tip, used in UAV helicopters, was designed, analyzed and additively manufactured. Aerodynamically, the unconventional blade shows better performance compared to the conventional blade at positive angles of attack. Acoustically, the unconventional blade showed a reduced noise level compared to the conventional blade. Acoustic testing of additively manufactured samples with five honeycomb core configurations showed higher performance for the 1.5 mm honeycomb cell samples 3D printed from T-PLA.

KEYWORDS: design, additive manufacturing, helicopter rotor blade, acoustic performance, CFD analysis

1. INTRODUCTION

A radio-controlled helicopter is an unmanned aircraft, controlled from the ground or from another aircraft, being in the UAV (Unmanned aerial vehicles) category. Radio-controlled helicopters are used to carry out a variety of missions: transport, human rescue, research of areas difficult to be reached by humans. UAV helicopter construction and structural parts are largely similar to those of pilot-controlled helicopters [1]. The wide areas of use of radio-controlled aircraft have led to the classification of radio-controlled helicopters according to rotor diameter into four categories [2]: micro radio-controlled helicopters (main rotor diameter 150 mm - 375 mm), mini radio-controlled helicopters (main rotor diameter 375 mm - 600 mm), medium radio-controlled helicopters (main rotor diameter 600 mm - 1100 mm) and large radio-controlled helicopters (main rotor diameter >1100 mm). The blades are parts of the structure of the helicopter that produce the lift needed to get it off the ground. They allow the radio-controlled helicopter to move horizontally, to hover at a fixed point and to move in several directions [3]. Helicopter blades depend on their shape, on the tip and on the material they are manufactured from. Due to the vibrations that occur, blade defects also result, which impair the operation of the helicopter. This is why many techniques have been developed to repair and maintain the blades. However, manufacturing also plays a key role, as it is in this process that blade performance is determined. Throughout the evolution of radio-controlled helicopters, a variety of materials have been used for blade structures: wood, metals, composites, reinforced plastic fibres and thermoplastic polymers.

Blades made of wood are strong, flexible, but their exposure to the environment results in their destruction due to adverse weather conditions (rain, wind, snow). The problem with wooden blades is that one blade absorbs more water than the other, resulting in vibrations during the flight. To prevent wood from warping, several wood fibres are laid out in layers and then glued together [4]. To prevent the problems caused by the wooden blades, they have been replaced by metal blades. This was an important step in the evolution of the helicopter, as it was no longer necessary to replace the whole set of blades since individual blades could now be replaced. The great disadvantage of metal blades (aluminium alloy) is that when a crack appears in a critical area, there is a possibility of catastrophic damage, leading to the helicopter crashing [5]. The use of composite materials in the blade structure has proven to be more efficient than wood or metal, both aerodynamically and structurally. While with metal, cracks would occur and advance leading to sudden destruction, the composite material signalled the occurrence of defects because they were visible. The applied load causes a crack in the structure of the composite material, but its propagation/stagnation is much slower compared to metallic materials. Fibres that do not undergo any changes take up the force and the crack does not advance, whereas steel allows the defect to develop in depth until the material breaks [4,5]. Additive manufacturing (3D printing) of blades allows cost savings and avoids material waste. Both the blades and the entire structure of the radio-controlled helicopter can be obtained by additive manufacturing [6]. Structures such as blade tips play a role in increasing lift by delaying boundary layer separation. The aerodynamics of the

radio-controlled helicopter is strongly influenced by the presence of these blade tips in the blade structure. Aerodynamic research and studies have shown different vortex development depending on the type of the blade tip used. Their design influences the performance of the helicopter, as the shape of the blade tip contributes to the control of vortex formation, noise reduction and reduction of vibrations, which occur due to lift asymmetry [7]. The tapered blade tip is predominantly used in Europe and is advantageous noise-wise as it reduces the noise level caused by the helicopter flight. However, the main disadvantage of this blade tip is that it cannot be used at high speeds [7]. The BERP (British Experimental Rotor Programme) blade tip is suitable for higher operating speeds than previous blade tips. It can be used both at low incidence angles and at high incidence angles without stall at high Mach numbers [8]. BERP type blade tips have numerous applications in both civil and military fields and are found in the structure of helicopters such as AgustaWestland AW101, Westland Lynx, Lockheed Martin VH-71 Kestrel.

In this paper, an unconventional blade structure with corrugations at the trailing edge and BERP type blade tip was designed, analysed (aerodynamically and acoustically) and additively manufactured. In addition, 3D-printed samples were also manufactured in order to obtain the acoustic performance of the honeycomb blade core with different variations of the core size.

2. EXPERIMENTAL SETUP

The SolidWorks 2021 software system was used to design the acoustically tested blades and samples. For the CFD (Computational Fluid Analysis) technique and acoustic simulation of the blades the SolidWorks 2021 software system, Flow Simulation module was used. In order to determine the equivalent stresses and total blade deformations the Ansys 16 software system was used. The FFF (Fused Filament Fabrication) or 3D printing process was used to obtain the designed samples that were acoustically tested. The designed samples and blade segments were fabricated by FFF using the Ultimaker S5 printer. The samples are tested in the acoustic impedance tube, also called Holmarc HO-ED-A-03, to obtain the absorption coefficient variation. An impedance tube consists of a cylindrical tube, inside which the 3D printed sample is placed; a loudspeaker, which is the sound generation source; a microphone; and a data acquisition system (Figure 1).

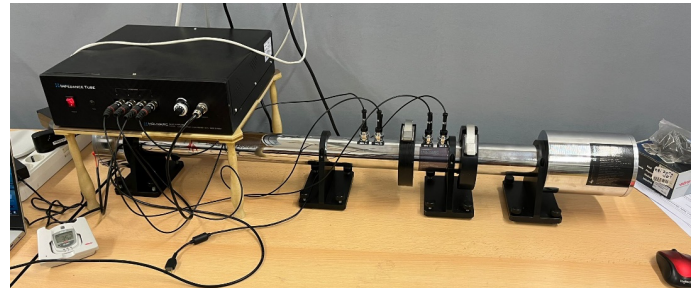


Figure 1. The impedance tube used for acoustic testing

3. UNCONVENTIONAL BLADE DESIGN

The UAV helicopter blades had the NACA 0012 profile. Three planes parallel to the initial plane are laid out over a length of 550 mm. At each plane, the blade is twisted by two degrees from its original structure. Its chord is constant over a length of 450 mm, then tapers. The size of the constant chord is 33 mm (Figure 2). The unconventional novelty added to the blade structure is the addition of blade corrugations on the trailing edge (Figure 3). The idea of adding these corrugations is based on the birds' plumage structure, which has excellent flying ability. The area of corrugation placement is the trailing edge, as the leading edge is a region more prone to impact or potential blade accidents. Therefore, it is necessary for the leading edge to be more resistant to shock or impact [9]. At the basis of the blade tip design is the BERP type blade tip, shown above, which has standard dimensions [7]. Eight corrugations were designed on the constant chord blade area with a corrugation length of 39.1 mm.

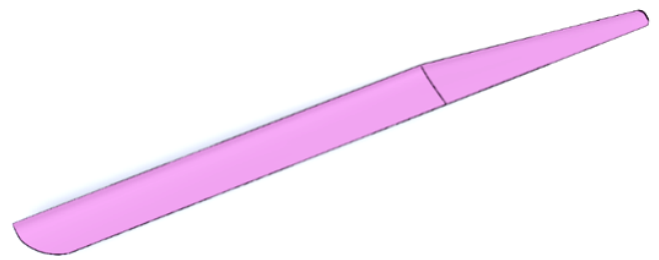


Figure 2. Design of the conventional blade

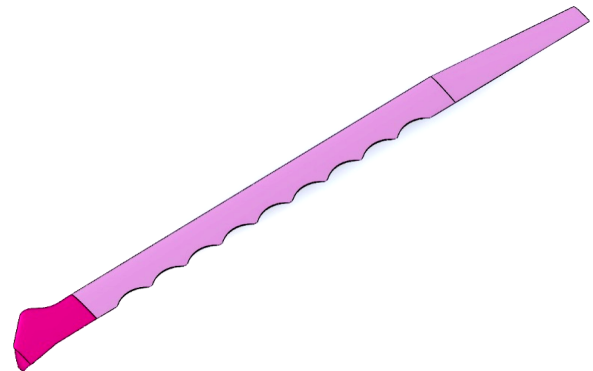


Figure 3. Design of the unconventional blade

4. CFD ANALYSIS OF THE BLADE

The CFD analysis of the blade allows the simulation of the air flow on the extrados of the blade, allowing to obtain the pressure and velocity distributed on the blade surface [10]. Depending on the angle of attack, three CFD analyses are performed, for the angles of attack (-5° , 0° , 10°), to observe the fluid behaviour when the angle is changed, for both types of blades (conventional blade and unconventional blade). Due to the uniformity of the exterior surface of the conventional blade (Figure 4), which has a conventional structure without corrugations or other unconventional elements, there are no discrepancies between the velocity and the theoretical fluid behaviour on the blade structure. The air foils move linearly and follow the path of the extrados.

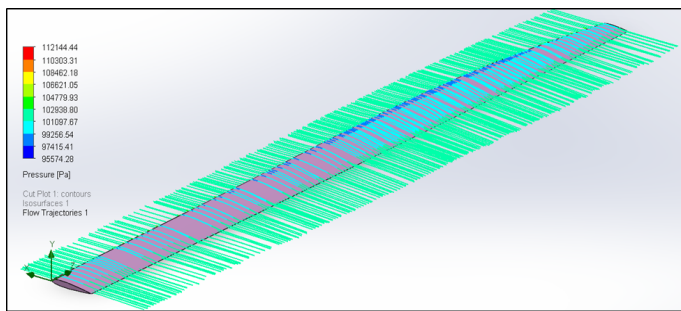


Figure 4. Pressure variation around conventional blade at 0° angle of attack

In contrast to the conventional blade at zero angle of attack, where the pressure at the leading edge is 101097.67 Pa, the pressure decreases for the corrugated blade in this area to 99226.27 Pa (Figure 5). At angle of attack equal to -5° , the pressure and velocity distribution changes. The maximum velocity value decreases and the air foils are more abruptly detached from the blade surface. The behaviour of velocity and pressure remains the same as for the analysis at zero angle of attack, but the described pressure field is slightly different.

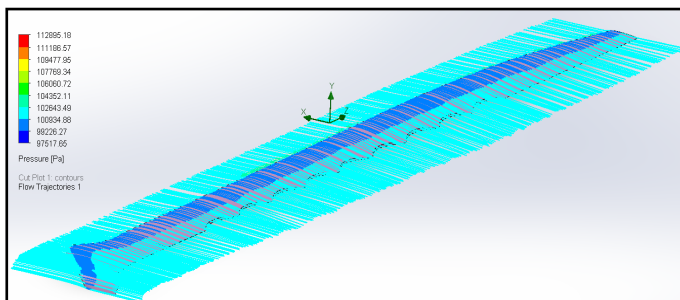


Figure 5. Pressure variation around unconventional blade at 0° angle of attack

When the angle of attack is increased by a positive value of 10° , a change in the behaviour of the fluid is observed, characterised by a decrease in the velocity on the extrados. The inclination of the blade caused by the increase in the angle of attack causes

the velocity on the blade surface to decrease. In contrast to situations where the angle of attack is zero or has a negative value, the pressure increases in the leading edge area towards the intrados to a value of about 105149.85 Pa. From the CFD analysis, the lift and drag values were extracted for each value of angle of attack (-5° , 0° , 10°) to determine the lift coefficient and drag coefficient for the 2 blade types (Table 1).

Table 1. Centralisation of lift and drag coefficient values as function of blade angle of attack

Blade type	Angle of attack	Lift coefficient	Drag coefficient
Conventional blade	0°	0.085	0.019
	-5°	0.012	0.01
	10°	0.258	0.087
Unconventional blade	0°	0.055	0.015
	-5°	0.007	0.012
	10°	0.269	0.088

These aerodynamic coefficients are intended to provide information on the performance of the 2 blade types. It can be concluded that the corrugations and blade tip are efficient only at high angles of attack, such as 10° . At zero angle of attack or negative angle of -5° , the conventional blade is more efficient because it results in a higher lift than the unconventional blade. For a UAV helicopter blade, these coefficients have small values because of the small lift area compared to an aircraft wing.

5. ACOUSTIC ANALYSIS OF THE BLADE

The noise produced by the helicopter during flight arises from several causes, such as the engine, but the dominant source is aerodynamic, as the interaction between fluid and blades takes place. The reduction of noise caused by the blades during rotation can be evaluated and determined by performing acoustic analysis of the blade, which provides information about the fluid flow on the blade surface and the noise level generated. In order to establish noise reduction solutions, it is necessary to know precisely the sources of the noise generation, which can be divided into two categories: the actual interaction of the fluid with the blade structure, which can be influenced by flight conditions, meteorological and atmospheric conditions; the noise produced by the blade in an undisturbed environment, which can generate vortices at the blade tip and in the trailing edge area [11]. As a result, the research conducted [12] resulted in the establishment of solutions to mitigate the noise caused: the choice of a different material, the arrangement of corrugations on the trailing edge of the blade due to vortices formed by the air flow on the blade and the design of a blade tip, which

ensures a laminar trajectory of the air foil and the minimization of vortex formation. The acoustic analyses of the conventional blade and the corrugated blade were performed in SolidWorks Flow to compare the results obtained, for a velocity of 80 m/s. In the acoustic analysis of the conventional blade, the sound level increases in the area where the profile chord is no longer constant and decreases, reaching values in the range 43.79-51.09 dB (Figure 6).

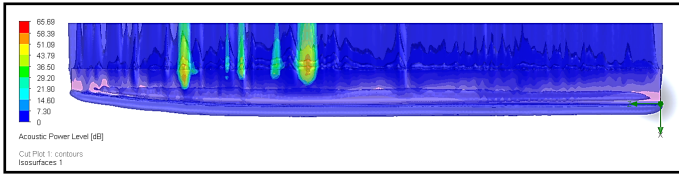


Figure 6. Acoustic analysis of the conventional blade

The addition of corrugations on the trailing edge caused these values to decrease by three times to values of 7.29-14.57 dB. Studies [7,11] have shown that the BERP blade tip arrangement reduces noise in the blade embedment area, as can be seen in Figure 7.

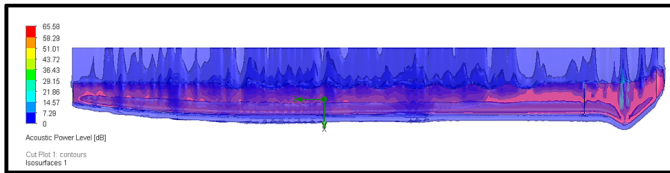


Figure 7. Acoustic analysis of the unconventional blade structure

The value of sound caused by aerodynamic reasons decreased for the unconventional blade by 0.11 dB. According to aviation regulations, the maximum permissible sound limit of the UAV helicopter is 87 dB. The conventional blade achieves a sound value of 65.69 dB and the unconventional one of 65.58 dB. The noise reduction is due to the placement of the corrugations on the trailing edge and the BERP blade tip. In conclusion, the conventional blade has disadvantages during helicopter flight, being noisier than the corrugated blade.

6. ADDITIVE MANUFACTURING OF THE SAMPLES

Three types of filaments (PLA - Polylactic Acid, CPE - Co-Polyester and T-PLA - Technical PLA) were used to determine the acoustic performance (Sound Absorption Coefficient and Sound transmission loss) of the 3D printed samples. For acoustic testing of the samples, it is necessary that the dimensions of the samples correspond to the dimensions of the impedance tube used. The height of the samples was 15 mm, the outer diameter 50.5 mm, and the shell size 1.5 mm. For the manufacture

of the acoustically tested samples, the 3D printing parameters were used (Table 2).

Table 2. 3D printing parameters used to manufacture the samples

3D printing parameters	Value		
	PLA	CPE	T-PLA
Infill density [%]	100	100	100
Nozzle diameter [mm]	0.4	0.4	0.4
Printing speed [mm/sec]	60	50	55
Layer height [mm]	0.1	0.1	0.15
Bed temperature [°C]	60	85	60
Printing temperature [°C]	200	240	210

Five samples with different honeycomb cell sizes were designed by modifying the circle inscribed in the hexagon (1.5 mm, 2 mm, 2.6 mm, 3.2 mm and 3.8 mm). The honeycomb structure is used inside the blade and undertakes aerodynamic, structural and acoustic loads. Figure 8 depicts the five blue CPE samples manufactured by the 3D printing process, varying the hexagonal core by enlarging the inscribed circle. The fabrication of the blue CPE filament samples took one day, 21 hours and 58 minutes. The mass of the CPE filament is 112 grams.

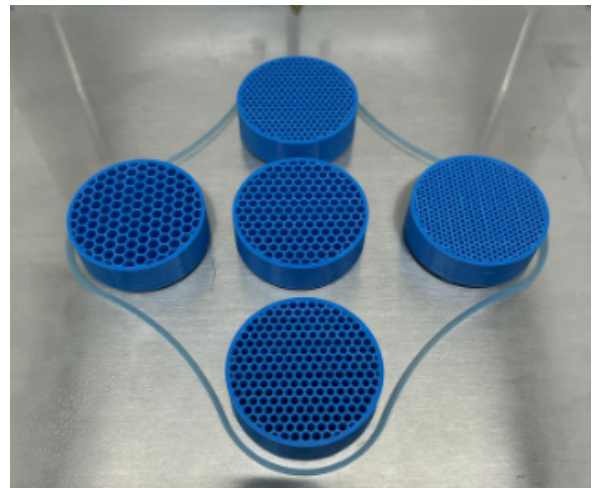


Figure 8. 3D printing of the CPE samples

7. ACOUSTIC TESTING OF THE SAMPLES

Noise pollution is one of the most common problems in aviation, the main source of which is aerodynamics. The rotation of helicopter blades causes changes in fluid behaviour, which generates sound during flight. The noise produced is a problem for the human factor, who can be significantly affected by this noise source. The aim is to mitigate the sound in order to comply with the rules imposed by aviation regulations [12,13]. Research has shown that sound reduction is an important goal in aviation and is influenced by several major factors [13-15]: materials and geometry of the aircraft structure; aerodynamic profile of the blade; blade dimensions. Noise mitigation caused by aircraft structures is an

important issue in aviation, as it is a dangerous factor for the health of the population, and it should comply with aviation legislation related to noise pollution. The materials that absorb sound best are porous materials [16-18], as opposed to solid materials. The sample (Figure 9) is placed inside the impedance tube, with the honeycomb structure facing the speaker, which generates the sound. Microphones are placed in the wall of the tube, which record the transmitted signal. Nine frequency values are set, in the range 500 Hz - 3150 Hz. The signals generated by the source contact the walls of the tube and the sound waves are reflected, transmitted or absorbed by the honeycomb structure. Recording the signals provides information about the loss of sound intensity and the variation of the absorption coefficient.

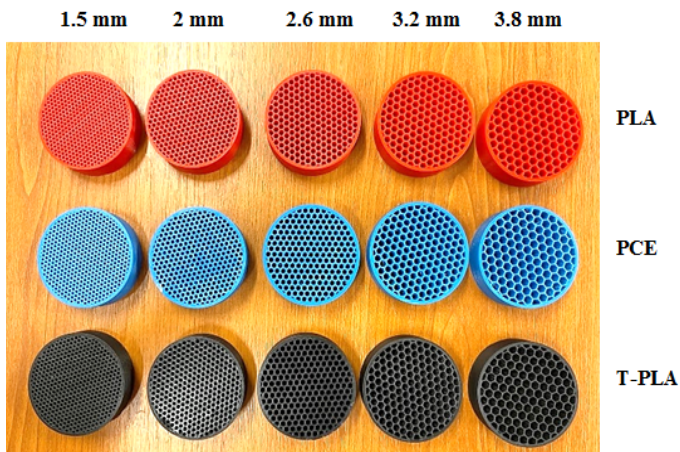


Figure 9. Variation of the pressure coefficient on the wing surface

From the acoustic tests of the 3D printed samples and from the absorption coefficient analysis (Figure 10, Figure 11 and Figure 12), the T-PLA material is the most efficient, because it shows the best acoustic performance. The absorption coefficient value ($\alpha=0.47$) is the highest for T-PLA, while the CPE material shows the low acoustic performance ($\alpha=0.45$).

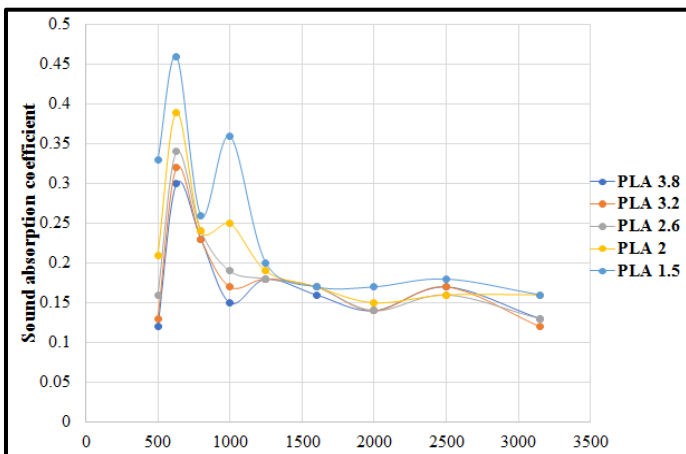


Figure 10. Variation of sound absorption coefficient - frequency for the PLA samples

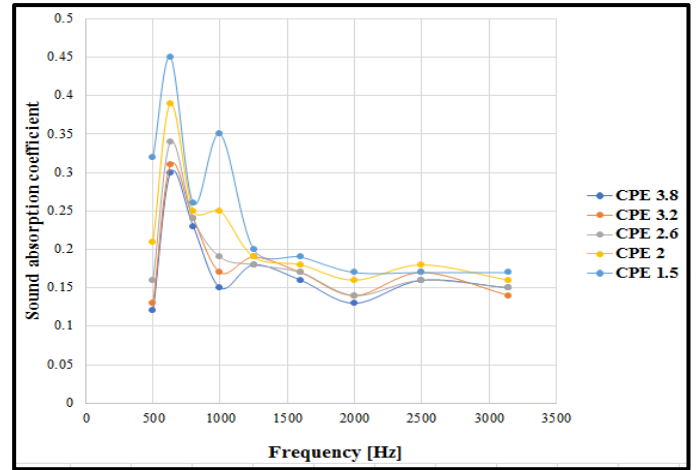


Figure 11. Variation of sound absorption coefficient - frequency for the CPE samples

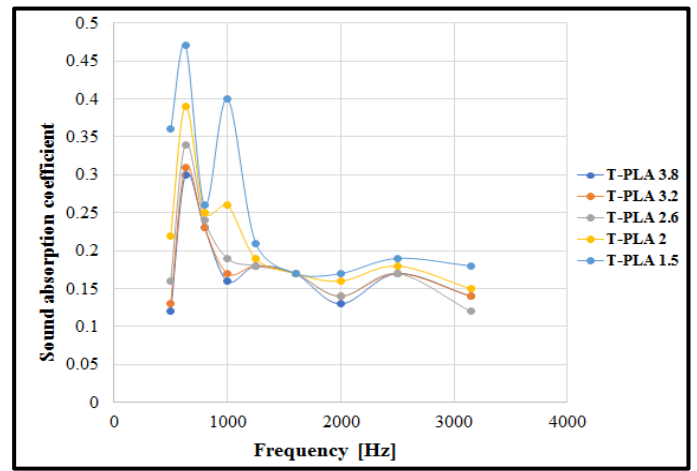


Figure 12. Variation of sound absorption coefficient - frequency for the T-PLA samples

In addition, the sound transmission loss (Figure 13, Figure 14 and Figure 15) is also the highest for the T-PLA material. From the acoustic analyses it was also concluded that samples with 1.5 mm honeycomb cell show the best acoustic performance, for all three types of materials (PLA - Polylactic Acid, CPE - Co-Polyester and T-PLA - Technical PLA). This may be due to the higher amount of material in the 1.5 mm cell samples, which absorbs sound better, but also to the denser porosity [19].

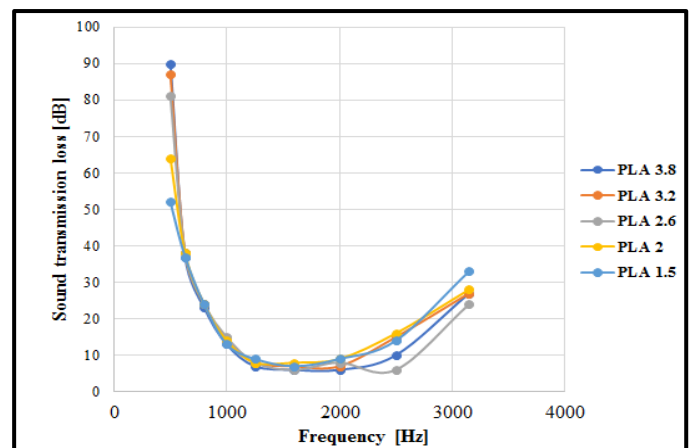


Figure 13. Variation of sound transmission loss – frequency for the PLA samples

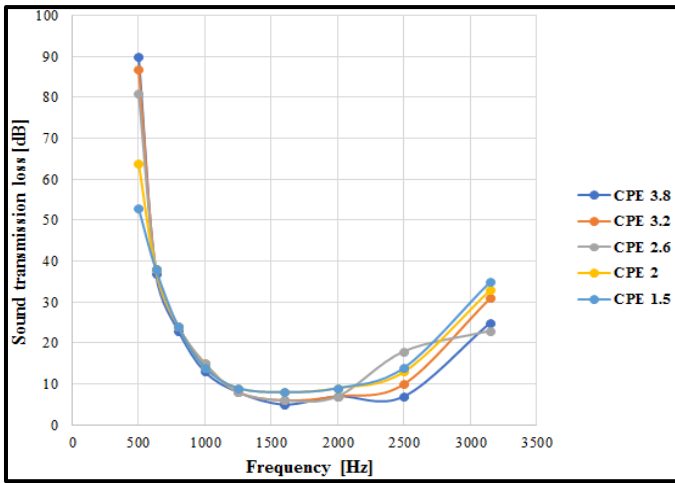


Figure 14. Variation of sound transmission loss – frequency for the CPE samples

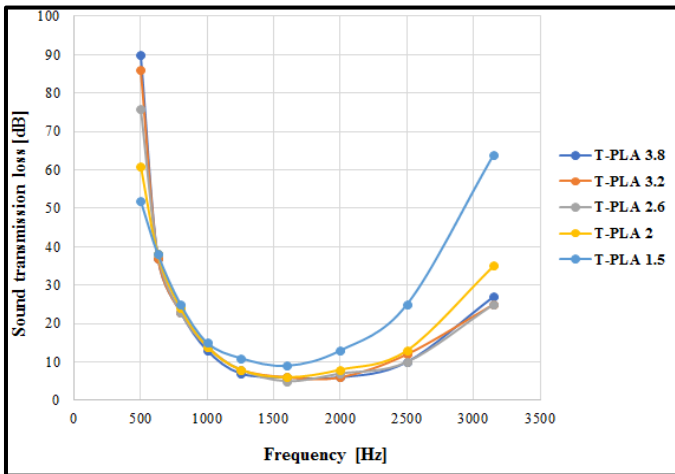


Figure 15. Variation of sound transmission loss – frequency for the T-PLA samples

8. ADDITIVE MANUFACTURING OF THE UNCONVENTIONAL BLADE

Based on the acoustic analysis of the 3D printed samples, it was found that the T-PLA filament exhibited both the best acoustic performance (sound absorption coefficient) and the fewest printing defects. Thus, the unconventional honeycomb core blade structure was made from T-PLA filament. The manufacture of the unconventional blade involves splitting the blade into three sections and the blade tip as shown in Figure 16. This sectioning was necessary to fit into the printing volume of the Ultimaker S5 printer.

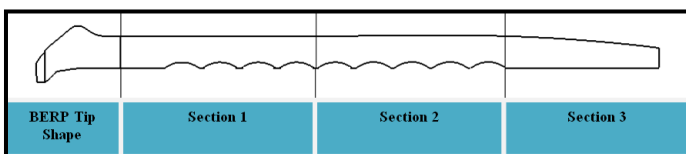


Figure 16. Unconventional blade sections required for 3D printing

3D printing of the blade sections was performed at the following parameters: infill density: 40%; layer thickness: 0.15 mm; inner space infill: tri-hexagonal configuration. The 3D printing time of the

unconventional blade sections was 28 hours and 47 minutes. The final shape (Figure 17) of the unconventional blade is obtained by gluing the blade sections with cyanoacrylate adhesive, adding the blade tip at the end.

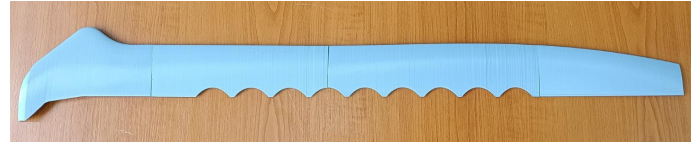


Figure 17. The final shape of the 3D printed unconventional blade

9. CONCLUSIONS

The blades of a UAV helicopter are the most important part of the structure of this flying machine, as their failure can cause serious consequences such as the helicopter crashing. By modifying the structure (arrangement of corrugations on the trailing edge) and adding a BERP-type blade tip, the following advantages and disadvantages of the unconventional blade were observed: it is acoustically efficient, as it reduces the noise caused, but it is aerodynamically inefficient, as it generates less lift than the conventional blade. Aircraft regulations impose a maximum permissible sound limit of 87 dB. Acoustic analysis of the blade showed that the corrugated blade generates a maximum sound of 65.58 dB, while the conventional blade produces sound of 65.69 dB. To further reduce the sound produced, the honeycomb core structure is integrated inside the blade, which absorbs sound waves better.

From an aerodynamic point of view, the lift generated by the conventional blade is higher than the one with corrugations on the trailing edge at zero angle of attack and negative -5° angle of attack, while at positive 10° angle of attack the unconventional blade produces more lift. Therefore, the unconventional blade is only effective when the angle of attack increases to positive values, where the helicopter requires more lift. The blade material is an important factor in the 3D printing of the blade, because it was found that of all the thermoplastic materials analysed (PLA - Polylactic Acid, CPE - Co-Polyester and T-PLA - Technical PLA), the T-PLA material is the most advantageous in terms of defects arising from 3D printing as well as from an acoustic point of view, because it has the highest sound wave absorption coefficient (samples with 1.5 mm honeycomb cell). In conclusion, it can be highlighted that this type of unconventional blades can be used in aviation, especially in UAV helicopters and can be very successful in terms of noise pollution reduction.

10. REFERENCES

1. Fahlstrom, P. G., Gleason, T. J., Sadraey, M. H. Introduction to UAV systems, John Wiley & Sons, (2022).
2. Lawrence, P., RC Helicopters: The Pilot's Essentials, CreateSpace Independent Publishing, (2017).
3. Rotaru, C., Todorov, M., Helicopter flight physics. Flight Physics-Models, Techniques and Technologies, IntechOpen, London, (2018).
4. Schafer, J., Helicopter Maintenance, Aviation Maintenance, (1986).
5. Federal Aviation Administration (FAA). Helicopter Instructor's Handbook (FAA-H-8083-4), https://www.faa.gov/regulations_policies/handbooks_manuals/aviation/media/FAA-H-8083-4.pdf.
6. Graba, M., Grycz, A., Assessment of the Mechanical Properties of Selected PLA Filaments Used in the UAV Project, Materials Vol.16, (2023).
7. Brocklehurst, A., Barakos, G.N., A review of helicopter rotor blade tip shapes, Progress in Aerospace Sciences, Vol. 56, pp. 35–74, (2013).
8. Marques, P., Maligno, A., Dierks, S., Penev, V., Bachouche, A., The Jinn military unmanned helicopter program: rotor blade tip aerodynamics of the advanced technology demonstrator, International Journal of Unmanned Systems Engineering., Vol.1, No.3, (2013).
9. Song, W., Mu, Z., Wang, Y., Zhang, Z., Zhang, S., Wang, Z., Li, B., Zhang, J., Niu, S., Han, Z., Ren, L., Comparative investigation on improved aerodynamic and acoustic performance of abnormal rotors by bionic edge design and rational material selection, Polymers, Vol. 14, No. 13, (2022).
10. Cao, H., Zhang, M., Cai, C., Zhang, Z., Flow topology and noise modeling of trailing edge serrations. Applied Acoustics, Vol. 168, (2020).
11. Yung, H.Y, Rotor Blade–Vortex Interaction Noise, Progress in Aerospace Sciences, Vol.36, pp. 97–115, (2000).
12. Lacagnina, G., Chaitanya, P., Kim, J.H., Berk, T., Joseph, P., Choi, K.S., Ganapathisubramani, B., Hasheminejad, S.M., Chong, T.P., Stalnov, O. Shahab, M.F., Leading edge serrations for the reduction of aerofoil self-noise at low angle of attack, pre-stall and post-stall conditions, International Journal of Aeroacoustics, Vol. 20, No. 1-2, pp.130-156, (2021).
13. Kessler, C., Active rotor control for helicopters: individual blade control and swashplateless rotor designs, CEAS Aeronautical Journal, Vol. 1, pp. 23-54, (2011).
14. Pakhov, V.V., Fayzullin, K.V. and Denisov, S.L., Measuring the acoustic characteristics of a helicopter rotormodel in a wind tunnel, Acoustical physics, Vol.66, pp.44-54, (2020).
15. Hu, Z., Liu, Y., Shi, Y. and Xu, G., An Experimental Study on Rotor Aerodynamic Noise Control Based on Active Flap Control, Aerospace, Vol. 10, No.2, (2023).
16. Ring, T.P., Langer, S.C., Design, Experimental and Numerical Characterization of 3D-Printed Porous Absorbers, Materials, Vol.12, (2019).
17. Monkova, K., Vasina, M., Monka, P.P., Vanca, J., Kozak, D., Effect of 3D-Printed PLA Structure on Sound Reflection Properties, Polymers, Vol. 14, (2022).
18. Zieliński, T.G., Dauchez, N., Boutin, T., Leturia, M., Wilkinson, A., Chevillotte, F., Bécot, F.X., Venegas, R., Taking advantage of a 3D printing imperfection in the development of sound-absorbing materials, Applied Acoustics, Vol. 197, pp. 108941, (2022).
19. Monkova, K., Vasina, M., Monka, P.P., Kozak, D., Vanca, J., Effect of the Pore Shape and Size of 3D-Printed Open-Porous ABS Materials on Sound Absorption Performance, Materials, Vol. 13, (2020).